

Particles separation in anisotropically confined two-dimensional multi-species systems

This article has been downloaded from IOPscience. Please scroll down to see the full text article.

2007 J. Phys.: Condens. Matter 19 356213

(<http://iopscience.iop.org/0953-8984/19/35/356213>)

View [the table of contents for this issue](#), or go to the [journal homepage](#) for more

Download details:

IP Address: 129.252.86.83

The article was downloaded on 29/05/2010 at 04:34

Please note that [terms and conditions apply](#).

Particles separation in anisotropically confined two-dimensional multi-species systems

Yanhong Liu and Lock Yue Chew

School of Physical and Mathematical Sciences, Nanyang Technological University, 637616, Singapore

Received 11 May 2007, in final form 23 July 2007

Published 8 August 2007

Online at stacks.iop.org/JPhysCM/19/356213

Abstract

Self-organized separation of multi-species charged particles in anisotropically confined two-dimensional systems is studied by means of molecular dynamics simulation. The multi-species particles of different mass and charge, interacting through a Coulomb potential, are confined by external potentials of different shapes, such as the circular, elliptical, triangular and square shaped potentials. It is found that the different particles segregate into different shells, with the particles having the largest (smallest) mass-to-charge ratio located nearest to (furthest away from) the system center. When the different particles possess the same mass-to-charge ratio, they become mixed together, despite having different mass and charge. This general rule is independent of the total number of particles, the number of species and the symmetries of the different confinement potentials. When these potentials rotate at a sufficiently high frequency around their origins, the anisotropy of the system configuration can be destroyed, and the whole system configuration becomes circular in shape, while the general rule of particle separation remains valid.

(Some figures in this article are in colour only in the electronic version)

1. Introduction

Many significant studies have been dedicated recently to two-dimensional (2D) clusters of a finite number of interacting particles subjected to an external confinement potential. Typical experimental examples of such 2D systems include electrons on the surface of liquid helium [1], electrons in quantum dots [2], colloidal suspensions [3], and confined plasma crystals [4–8]. Most of the previous studies have been performed by considering the particles in an isotropic confinement potential [9–13]. In an isotropic confinement potential, a circular shell structure is obtained and a Mendeleev-type of table for the structures is constructed [13–15].

In some experiments, however, the external confinement potential is not isotropic. For example, anisotropic confinement potentials of elliptical, triangular and square shapes have been explored in quantum dots [16–19]. Such investigation has found that the states of electrons

in a triangular quantum dot are slightly stable compared to that in a circular quantum dot due to the effect of geometry [18]. In addition, an interesting relation between the quantum and classical charge distributions in an anisotropic potential has also been established [19] at high magnetic field, whereupon the quantum charge density tends to reproduce simultaneously all the degenerate lowest-energy classical configurations. Studies are also carried out to investigate the phase transition and excitation spectrum of classical 2D charged systems in circular and elliptical potentials. These studies have uncovered that changing the eccentricity of the elliptical confinement potential can induce phase transition in the systems [20–22]. Research on Bose–Einstein condensation (BEC) has also employed anisotropic potentials such as the elliptical potential [23–25]. As the elliptical confinement potential is rotated about its origin, a vortex lattice is found to form as a result of dynamical instability which occurs during the evolution of the condensate [23–27].

In all the above studies, only a single species of particle is considered. In real experiments, however, it is very likely that more than one species of particles exist in the systems [28–37]. Mangold *et al* [28] have studied experimentally the melting behavior of a binary system of paramagnetic colloidal spheres with different sizes confined in 2D circular cavities in an external magnetic field. They found that the melting process takes place in several stages where first the small particles and afterwards the big particles become delocalized. Nelissen *et al* [29] has also investigated numerically the induced order and re-entrant melting in a binary system of classical charged particles interacting through a dipole repulsive potential and confined in a 2D circular hard-wall trap. They found that the presence of small particles stabilizes the angular order of the system as a consequence of radial fluctuations of the small particles. Grzybowski *et al* [30, 31] have studied experimentally a 2D system of ferromagnetic particles (disks) with two different sizes trapped in a liquid–air interface and confined by an external magnetic field. They have found that the particles of different sizes can either separate or mix together, depending on the experimental conditions in the isotropically confined system. Recently, the self-organizing structure of a 2D system containing more than one species of charged particles has been studied [32–35]. The studies have found that in an isotropic (circular) confinement potential, the particles of different species segregate into different shells, with the particles of the largest (smallest) mass-to-charge ratio tending to populate near to (far away from) the system center [35]. The different particles also become mixed together if they have the same mass-to-charge ratio, although their individual masses and charges [34, 35] are different. The investigation performed so far on 2D multi-species systems has been restricted to confinement in an isotropic potential. It will be interesting to investigate the self-organizing structures and the general conditions of possible species separation of these systems as they are confined in different anisotropic external potentials, such as the elliptical, triangular and square shaped potentials. The effect of rotation of these anisotropic potentials on the overall system structure, as well as the species separation within the systems, will also be examined in this paper.

The paper is organized as follows. In section 2, we first present our model system and numerical simulation approach. Then, in section 3, we discuss and compare the different minimum energy configurations obtained for the two-species and three-species charged particles as they are confined within circular, elliptical, triangular and square shaped potentials. The effect of rotations of these external confinement potentials on the system structures will also be discussed in this section. Finally, section 4 concludes the paper.

2. Model system and numerical approach

We consider a 2D system consisting of a finite number (N) of charged particles interacting through a Coulomb potential. The particles are, in addition, confined within an external

potential which is either circular, elliptical, triangular or square in shape [18–21, 25, 32–35, 38]. The Hamiltonian of the system is $H = K + U$, where K is the kinetic energy and

$$U = \sum_{i=1}^N \frac{1}{2} M_i^{(k)} \omega_0^2 (\alpha x_i^2 + y_i^2) (1 + \beta) + \frac{1}{\varepsilon} \sum_{i < j}^N \frac{Q_i^{(k)} Q_j^{(k)}}{|\mathbf{r}_i - \mathbf{r}_j|} \quad (1)$$

is the potential energy. In equation (1), $M_i^{(k)}$ and $Q_i^{(k)}$ are the respective effective mass and charge of the particle i with position coordinates $\mathbf{r}_i = (x_i, y_i)$ belonging to species k ; ω_0 is the trapping frequency of the external potential whose anisotropy is described by the parameters α and β —employed to specify the elliptical, triangular and square shaped potentials; and ε is the dielectric constant of the surrounding medium. The potential energy given in equation (1) can also be written in dimensionless form as follows:

$$U = \sum_{i=1}^N m_i^{(k)} (\alpha x_i^2 + y_i^2) (1 + \beta) + \sum_{i < j}^N \frac{q_i^{(k)} q_j^{(k)}}{|\mathbf{r}_i - \mathbf{r}_j|}, \quad (2)$$

where the mass and charge are normalized by that of the first ($k = 1$) species, and the space coordinate and energy are normalized by $r_0 = (2Q^{(1)2}/M^{(1)}\varepsilon\omega_0^2)^{1/3}$ and $E_0 = M^{(1)}\omega_0^2 r_0^2/2$, respectively. Without loss of generality, we have dropped the particle index i in $Q_i^{(k)}$ and $M_i^{(k)}$, since particles of the same species are indistinguishable. For convenience, we have also introduced the species mass-to-charge ratio $s^{(k)} = m^{(k)}/q^{(k)}$, such that $s^{(1)} = 1$ in this paper.

In order to have external confinement potentials of different shape, we choose the parameters α and β as follows: (1) for a circular potential, $\alpha = 1$ and $\beta = 0$; (2) for an elliptical potential, $\alpha = 0.5$ and $\beta = 0$; (3) for a triangular potential, $\alpha = 1$ and $\beta = 2 \cos(3\phi)/7$ [18]; and (4) for a square potential, $\alpha = 1$ and $\beta = \cos(4\phi)/5$ [19]. Here, ϕ is the angle made by the position vector of a particle at \mathbf{r} with respect to the x -axis in the x - y plane. For studying the rotational effect of the external confinement potential, we replace the x_i and y_i in equations (1) and (2) by $(x_i \cos(\Omega t) + y_i \sin(\Omega t))$ and $(-x_i \sin(\Omega t) + y_i \cos(\Omega t))$ respectively, where Ω is the rotation frequency of the potential, and t is the time. Note that Ω and t have been normalized by $\Omega_0 = \omega_0/\sqrt{2}$ and $t_0 = \sqrt{2}/\omega_0$, respectively.

We simulate the motion of the charged particles by molecular dynamics (MD). To achieve the state of minimum energy (at which $H \rightarrow U$), each run is started with random initial spatial and velocity distributions that are set at a high temperature ($T = 0.05 \rightarrow 1.0$, where T has been normalized by E_0). The system is then slowly annealed until the temperature reaches zero ($T = 0 \pm 10^{-6}$). The annealing time is $6 \times 10^4 \omega_0^{-1}$, and the integration time step is $0.003 \omega_0^{-1}$. We have checked the accuracy of our simulations by comparing our results to the stable-state configurations of single- or two-species clusters obtained from Monte Carlo (MC) or MD simulations [20, 21, 32, 34]. We found very good agreement between our results and those obtained from these MC and MD simulations.

3. Simulation results

3.1. Systems with two species of particles

3.1.1. Different mass. We consider a system consisting of two species of $N = 100$ particles with different mass but the same charge ($q^{(2)} = q^{(1)} = 1.0$) being confined in circular (for comparison with the anisotropic potential), elliptical, triangular and square shaped potentials. Figure 1 shows the minimum energy configurations of the two-species systems. The subfigures are arranged such that the columns show the effect of mass $m^{(2)}$, while the rows show the effect of the confinement potentials of different shape on the system structures. From figure 1,

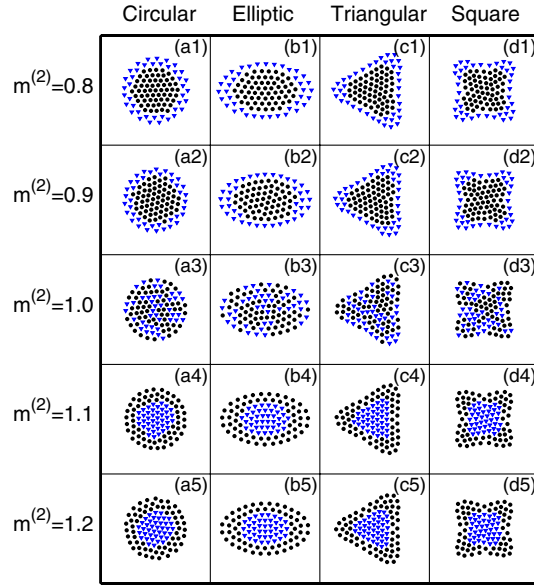


Figure 1. The minimum energy configurations for two species of particles with different masses but the same charge $q^{(1)} = q^{(2)} = 1.0$. These particles are confined within circular, elliptic, triangular and square shaped potentials. The total number of particles is $N = 100$, and the number of particles for species 1 (dots) and 2 (triangles) are $N^{(1)} = 60$ and $N^{(2)} = 40$, respectively. All subfigures are in the same arbitrary scale.

one observes that, when $m^{(2)} \neq m^{(1)}$, particles of different mass segregate into different shells. On the other hand, when $m^{(2)} = m^{(1)}$, the different particles become mixed together, and are not physically separated. The shape of the whole system resembles the shape of the equipotential lines of the external confinement potentials [18, 19]. When $m^{(2)} = 0.8$ (figures 1(a1), (b1), (c1) and (d1)), particles of species 1 populate the system center and form a core surrounded by a shell of particles of species 2; when $m^{(2)} = 0.9$, the shell of particles of species 2 assemble themselves closer to the central core formed by species 1; when $m^{(2)} = 1.0$, the two species become mixed together; when $m^{(2)} = 1.1$, the two species separate again, but now particles of species 2 form the central core surrounded by a shell of particles of species 1; when $m^{(2)} = 1.2$, the central core formed by species 2 becomes more compact with species 1 still surrounding it.

These results can be understood from the fact that the organization of the whole system configuration is determined by the competition between two types of forces: the force caused by the inward mass-dependent confinement potential, and the charge-dependent repulsive force acting between the particles. The inward mass-dependent confinement force pushes the particles into the system center, while the charge-dependent inter-particle repulsive force prevents the charged particles from moving too close to each other. When species 1 and 2 possess the same charge $q^{(2)} = q^{(1)} = 1.0$, the particle with the larger mass feels a relatively strong inward confinement force, and hence is pushed near to the system center in such a way that the total system energy is minimized.

For the anisotropic potentials, the shell surrounding the central core is observed to be non-uniform in width as the particles tend to situate at the extreme positions—for example, at the corners of the triangular and square shaped systems. This is due to the fact that the particles feel less inter-particle repulsive force at the corners. Hence, occupying these regions has the effect

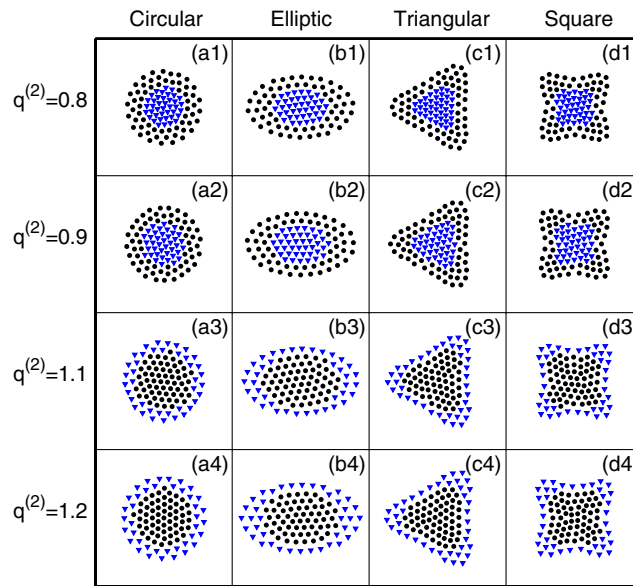


Figure 2. The minimum energy configurations for two species of particles with different charge but the same mass $m^{(1)} = m^{(2)} = 1.0$. These particles are confined within circular, elliptical, triangular and square shaped potentials. The total number of particles is $N = 100$, and the number of particles for species 1 (dots) and 2 (triangles) are $N^{(1)} = 60$ and $N^{(2)} = 40$, respectively. All subfigures are in the same arbitrary scale.

of reducing the whole system energy. We also observe from figures 1(d1)–(d5) that the system shape does not correspond to the equipotential lines (see [18] and [19]) of the confinement potential. We deem that this is a consequence of the strong inter-particle repulsive force. We prove our conjecture by simulating a system containing different particles interacting through a screened Coulomb potential, and obtain the expected resemblance of the system shape to the equipotential lines of the confinement potentials.

From these results, we observe that particles of the same charge but different mass separate into different shells, with particles having the largest (smallest) mass locate near to (far away from) the system center as they are being acted on by isotropic or anisotropic potentials.

3.1.2. Different charge. Next, let us consider the situation when the two species of particles have the same mass but different charges. The minimum energy configurations for this case are shown in figure 2, whose subfigures are arranged such that the columns show the effect of the charge $q^{(2)}$, while the rows show the effect of the different confinement potentials. From figure 2, one observes again a common feature among the different confinement potentials: particles of different species separate into different shells, with the particles of smaller (larger) charge locate near to (far away from) the system center. When $q^{(2)} = 0.8$, particles of species 2 are found near to the system center, while particles of species 1 form a shell around it. When $q^{(2)} = 0.9$, the central core of species 2 grows larger. It is still being surrounded by particles of species 1. When $q^{(2)} = 1.1 (> q^{(1)})$, species 2 begins to move away from the system center. They surround species 1, which now locates near to the system center. When $q^{(2)} = 1.2$, the system size has increased, with species 1 staying as the central core while being surrounded by a shell of particles formed by species 2. Thus, the particles arrange themselves according to the competing actions between the two forces: the inward mass-dependent confinement force

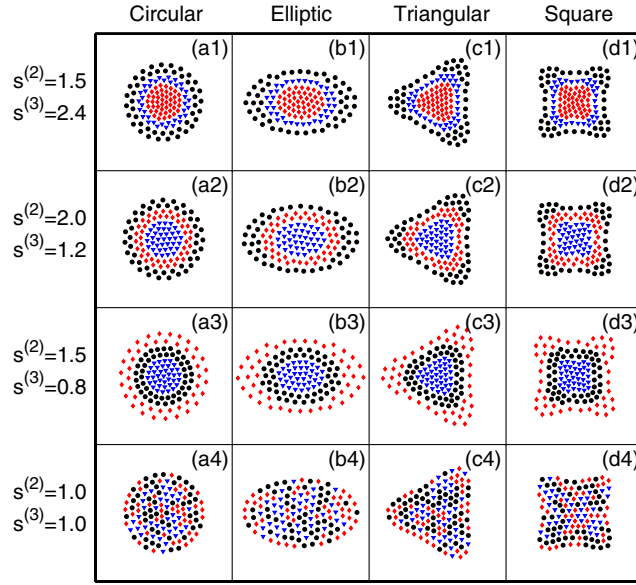


Figure 3. The minimum energy configurations for three species of particles with different mass-to-charge ratios (the masses and charges are different). These particles are confined within circular, elliptical, triangular and square shaped potentials. The total number of particles is $N = 130$, and the numbers of particles for species 1 (dots), 2 (triangles) and 3 (diamonds) are $N^{(1)} = 47$, $N^{(2)} = 38$ and $N^{(3)} = 45$, respectively. The masses and charges of species 2 and 3 in the subfigures are given as follows: in (a1), (b1), (c1) and (d1), $m^{(2)} = 1.2$, $q^{(2)} = 0.8$, $m^{(3)} = 2.4$ and $q^{(3)} = 1.0$; in (a2), (b2), (c2) and (d2), $m^{(2)} = 2.4$, $q^{(2)} = 1.2$, $m^{(3)} = 1.1$ and $q^{(3)} = 0.9$; in (a3), (b3), (c3) and (d3), $m^{(2)} = 1.3$, $q^{(2)} = 0.9$, $m^{(3)} = 1.2$ and $q^{(3)} = 1.5$; in (a4), (b4), (c4) and (d4), $m^{(2)} = 1.2$, $q^{(2)} = 1.2$, $m^{(3)} = 0.8$ and $q^{(3)} = 0.8$. All subfigures are in the same arbitrary scale.

and the repulsive force acting between the particles. When the two species have the same mass $m^{(2)} = m^{(1)} (= 1.0)$, particles with the larger charge feel a stronger inter-particle repulsive force, and are pushed far away from the system center in order to decrease the whole system energy, with the system center being occupied by particles of smaller charge. As the charge of a particular species increases, this species will experience a much stronger inter-particle repulsive force and is pushed much farther away from the system center, with a corresponding increase in the overall system size. This occurs when $q^{(2)} = 1.2$.

The above results show that particles with a smaller (larger) charge tends to situate near to (far away from) the system center when they possess the same mass. This is consistent with the general rule obtained in [35] for a circularly confined system. Here, we observe in addition that different particle species can be separated into different shells when confined by anisotropic potentials. Thus, the general rule for particle separation continues to apply within anisotropically confined systems.

3.2. Systems with three species of particles

Let us now extend the number of species to three and consider an $N = 130$ system. Figure 3 shows the minimum energy configuration of such a system with each species of particle having different mass and charge. The subfigures are arranged such that the columns show the effect of the particle mass-to-charge ratios $s^{(k)} = m^{(k)}/q^{(k)}$ ($k = 1, 2$ and 3), while the rows show the effect of the shape of the confinement potentials on the system structures. Interestingly, figure 3

shows that different particles separate into different shells, and the separation is determined by the mass-to-charge ratio: particles having the largest (smallest) mass-to-charge ratio situate nearest to (furthest away from) the system center. In figures 3(a1), (b1), (c1) and (d1), when $s^{(1)} < s^{(2)} < s^{(3)}$, particles of species 1, 2 and 3 are found to locate in the outer, middle and inner shells, respectively. In figures 3(a2), (b2), (c2) and (d2), when $s^{(1)} < s^{(3)} < s^{(2)}$, particles of species 1, 2 and 3 are found to locate in the outer, inner and middle shells, respectively. In figures 3(a3), (b3), (c3) and (d3), when $s^{(3)} < s^{(1)} < s^{(2)}$, particles of species 1, 2 and 3 are found to locate in the middle, inner and outer shells, respectively. Finally, in figures 3(a4), (b4), (c4) and (d4), when the different particles have the same mass-to-charge ratio $s^{(1)} = s^{(2)} = s^{(3)}$, the particles are found to mix together despite having different mass and charge. Through varying the mass-to-charge ratio of each species, we find that the particles can be placed in the inner, middle and outer shells of the system. These results can again be attributed to a consequence of the competitive effects between the inward mass-dependent confinement force and the repulsive force acting between the particles.

We have also considered multi-species systems with more than three species of particles in systems which contain a large number of particles, and found that the general rule of particle separation continues to apply. This general rule is indeed independent of the total number of particles and species, as well as the symmetries of the systems. Our results enable us to conclude that the unique dependence of the particle distribution on the mass-to-charge ratio observed for the multi-species systems in an isotropic confinement potential in [35] remains valid in the case of an anisotropically confined systems.

3.3. The effect of rotation of the confinement potentials on the system structures

In the studies on BEC under an anisotropic confinement potential rotating at a sufficiently high frequency, it was found that the initial elliptically shaped system can become deformed into a circular shape, with the production of a vortex lattice at the same time [23–27]. The rotation can be simply induced by physical means such as an external magnetic field [26, 27]. In the same vein, we would like to investigate the effect of the rotation of different external confinement potentials on the system structures of the multi-species systems. Figure 4 shows the minimum energy configurations of the systems confined by the rotating circular, elliptical, triangular and square shaped potentials with different rotation frequency Ω . From figure 4, we observe that the system configuration is not affected by a rotating circular confinement potential (figures 4(a1)–(a5)). On the other hand, at a sufficiently high rotational frequency, a rotating anisotropic confinement potential can lead to a minimum energy configuration that is circular in shape. For example, when $\Omega = 0.01$ (figures 4(b1), (c1) and (d1)), the shape of the system configuration is found to follow the equipotential lines of the confinement potentials; when $\Omega = 0.05$ (figures 4(b2), (c2) and (d2)), the shape of the system configuration becomes deformed and approaches the shape of a circle; when Ω is increased from 0.1 to 0.3, the system configuration becomes circular in shape (in figures 4(b5), (c5) and (d5)), i.e. the anisotropy of the system configuration has been destroyed by the rotation of the external confinement potentials. Remarkably, the general rule of particles separation remains valid within these rotating systems—particles from different species segregate into different shells, with particles of the largest (smallest) mass-to-charge ratio located nearest to (furthest away from) the system center.

These results can be understood from the fact that, as the external confinement potential is rotating around its origin, the different particles feel a time-dependent potential at a fixed position. When the rotation frequency is low, the particles can follow the potential variation, and arrange themselves in a shape resembling the equipotential lines of the confinement

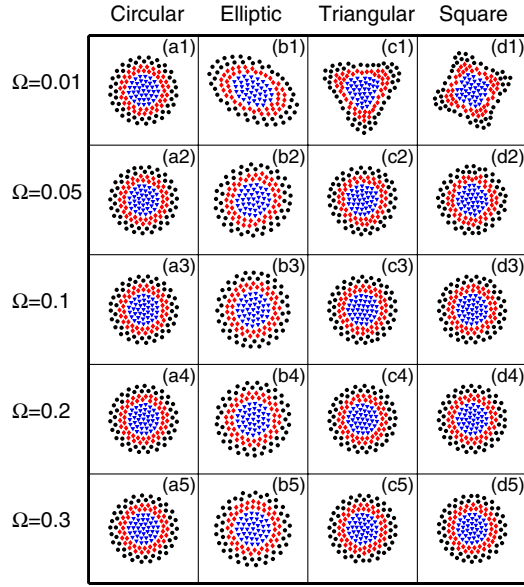


Figure 4. The minimum energy configurations for three species of particles confined within circular, elliptical, triangular and square shaped potentials which rotate with frequency Ω . The total number of particles is $N = 130$, and the number of particles for species 1 (dots), 2 (triangles) and 3 (diamonds) is $N^{(1)} = 47$, $N^{(2)} = 38$ and $N^{(3)} = 45$ respectively. In all the subfigures, the mass and charge of the particles are: $m^{(2)} = 2.4$, $q^{(2)} = 1.2$, $m^{(3)} = 1.1$ and $q^{(3)} = 0.9$. All subfigures are in the same arbitrary scale.

potential. When the rotation frequency is increased to a sufficiently high level, the particles (at a low temperature) can no longer follow the potential variation. Instead, the particles at different locations feel a time-averaged (i.e. effectively isotropic) confinement potential. Therefore, the final system configuration is circular in shape. The rotation frequency that is required to destroy the anisotropy of the system configuration is found to be inversely proportional to the mass of the particles in the system. This is because particles with a larger mass have a larger inertia, and hence have a longer response time when following the potential variation within a rotating confinement potential. We have verified this fact in a system containing particles with larger mass, for example, $m^{(2)} = 19.2$ and $m^{(3)} = 8.8$. Indeed, the system configuration becomes circular in shape at a much lower rotation frequency of $\Omega = 0.01$ for this system.

Finally, we observe from figures 4(a5), (b5), (c5) and (d5) that the size of the system configuration confined by a rotating elliptical potential is the largest. This is due to the fact that, for the elliptical system, the trapping frequencies are chosen as $\omega_x = 0.7\omega_0$ and $\omega_y = \omega_0$ in the x and y directions, respectively. Thus, the particles feel a smaller time-averaged confinement force, leading to a final system size that is larger than the other systems.

4. Conclusions

In conclusion, we have determined the minimum energy configurations of a multi-species system of charged particles interacting through a Coulomb repulsive potential confined by isotropic (circular) and anisotropic (elliptical, triangular and square) potentials by means of MD simulation. We have demonstrated that the general rule for particle separation obtained in reference [35] continues to apply within anisotropically confined systems: the larger the

mass-to-charge ratio, the closer the particles are to the system center. This rule is found to be independent of the total number of particles, the number of species and the symmetries of the system. When the anisotropic confinement potential rotates, the anisotropically shaped system can become deformed and circular in shape at a sufficiently high rotation frequency. In addition, the general rule of particle separation remains valid within these rotating systems. The rotation frequency required to destroy the anisotropy of the systems is found to be inversely proportional to the particle mass in the systems. It should be pointed out that these results are valid for a trapping potential that is quadratic in nature (refer to the potential energy term in equation (1)). In the single species case, the importance of the mass-to-charge ratio $s^{(k)}$ on the particle distribution is obvious, even during the stage of dynamical evolution. However, the importance of $s^{(k)}$ for a multi-species system is not evident, especially within anisotropically confined systems. An analytical investigation of the minimum energy particle distribution would thus be desirable, and our numerical results here would provide a good guide for such an analysis. Our results may also be useful for understanding many cluster and crystal models based on the quadratic confinement potentials, such as in some ferromagnetic particle systems [30, 31] and laser-cooled ionic systems [39–42].

Acknowledgment

Y H Liu gratefully acknowledges financial support from Nanyang Technological University.

References

- [1] Grimes C C and Adams G 1979 *Phys. Rev. Lett.* **42** 795
- [2] Ashoori R C 1996 *Nature* **379** 413
- [3] Golosovsky M, Saado Y and Davidov D 2002 *Phys. Rev. E* **65** 061405
- [4] Chu J H and I L 1994 *Phys. Rev. Lett.* **72** 4009
- [5] Thomas H, Morfill G E, Demmel V, Goree J, Feuerbacher B and Möhlmann D 1994 *Phys. Rev. Lett.* **73** 652
- [6] Melzer A, Nunomura S, Samsonov D and Goree J 2000 *Phys. Rev. E* **62** 4162
- [7] Liu B and Goree J 2005 *Phys. Rev. Lett.* **94** 185002
- [8] Liu Y H, Liu B, Chen Y P, Yang S Z, Wang L and Wang X G 2003 *Phys. Rev. E* **67** 066408
- [9] Kong M, Vagov A, Partoens B, Peeters F M, Ferreira W P and Farias G A 2004 *Phys. Rev. E* **70** 051807
- [10] Schweigert V A and Peeters F M 1995 *Phys. Rev. B* **51** 7700
- [11] Koulakov A A and Shklovskii B I 1998 *Phys. Rev. B* **57** 2352
- [12] Schweigert I V, Schweigert V A and Peeters F M 2000 *Phys. Rev. Lett.* **84** 4381
- [13] Bedanov V M and Peeters F M 1994 *Phys. Rev. B* **49** 2667
- [14] Block M, Drakoudis A, Leuthner H, Seibert P and Werth G 2000 *J. Phys. B: At. Mol. Opt. Phys.* **33** L375
- [15] Kong M, Partoens B and Peeters F M 2003 *New J. Phys.* **5** 23
- [16] Slachmuylders A F, Partoens B and Peeters F M 2005 *Phys. Rev. B* **71** 245405
- [17] Baelus B J and Peeters F M 2002 *Phys. Rev. B* **65** 104515
- [18] Ezaki T, Mori N and Hamaguchi C 1997 *Phys. Rev. B* **56** 6428
- [19] Szafran B, Peeters F M, Bednarek S and Adamowski J 2004 *Phys. Rev. B* **69** 125344
- [20] Cândido L, Rino J, Studart N and Peeters F M 1998 *J. Phys.: Condens. Matter* **10** 11627
- [21] Apolinario S W S, Partoens B and Peeters F M 2005 *Phys. Rev. E* **72** 046122
- [22] Schiffer J P 1993 *Phys. Rev. Lett.* **70** 818
- [23] Madison K W, Chevy F, Bretin V and Dalibard J 2001 *Phys. Rev. Lett.* **86** 4443
- [24] Feder D L, Svidzinsky A A, Fetter A L and Clark C W 2001 *Phys. Rev. Lett.* **86** 564
- [25] Lobo C, Sinatra A and Castin Y 2004 *Phys. Rev. Lett.* **92** 020403
- [26] Madison K W, Chevy F, Wohlleben W and Dalibard J 2000 *Phys. Rev. Lett.* **84** 806
- [27] Chevy F, Madison K W and Dalibard J 2000 *Phys. Rev. Lett.* **85** 2223
- [28] Mangold K, Birk J, Leiderer P and Bechinger C 2004 *Phys. Chem. Chem. Phys.* **6** 1623
- [29] Nelissen K, Partoens B, Schweigert I and Peeters F M 2006 *Europhys. Lett.* **74** 1046
- [30] Grzybowski B A, Jiang X, Stone H A and Whitesides G M 2001 *Phys. Rev. E* **64** 011603

- [31] Grzybowski B A, Stone H A and Whitesides G M 2000 *Nature* **405** 1033
- [32] Drocco J A, Reichhardt C J O, Reichhardt C and Jankó B 2003 *Phys. Rev. E* **68** 060401
- [33] Nelissen K, Partoens B and Peeters F M 2004 *Phys. Rev. E* **69** 046605
- [34] Ferreira W P, Munarin F F, Nelissen K, Filho R N C, Peeters F M and Farias G A 2005 *Phys. Rev. E* **72** 021406
- [35] Liu Y H, Chen Z Y, Yu M Y, Wang L and Bogaerts A 2006 *Phys. Rev. E* **73** 047402
- [36] Luo H and Yu M Y 1992 *Phys. Fluids B* **4** 3066
- [37] Ma J X, Liu J Y and Yu M Y 1997 *Phys. Rev. E* **55** 4627
- [38] Jean M S and Guthmann C 2002 *J. Phys.: Condens. Matter* **14** 13653
- [39] Tan J N, Bollinger J J, Jelenkovic B and Wineland D J 1995 *Phys. Rev. Lett.* **75** 4198
- [40] Mitchell T B, Bollinger J J, Itano W M and Dubin D H E 2001 *Phys. Rev. Lett.* **87** 183001
- [41] Hornekaer L, Kjergaard N, Thommesen A M and Drewsen M 2001 *Phys. Rev. Lett.* **86** 1994
- [42] Ostendorf A, Zhang C B, Wilson M A, Offenberg D, Roth B and Schiller S 2006 *Phys. Rev. Lett.* **97** 243005